Journal for ImmunoTherapy of Cancer

Clinicopathological and predictive value of MAIT cells in non-small cell lung cancer for immunotherapy

Lin Shi,[1,2] Jinying Lu,[2,3] Da Zhong,[2] Meijuan Song,[4] Jian Liu,[2,3] Wenhua You,[2,3] Wen-Hui Li,[5] Lin Lin,[6] Dongyan Shi,[2] Yun Chen [1,2,3]

To cite: Shi L, Lu J, Zhong D, *et al*. Clinicopathological and predictive value of MAIT cells in non-small cell lung cancer for immunotherapy. *Journal for ImmunoTherapy of Cancer* 2023;**11**:e005902. doi:10.1136/jitc-2022-005902

► Additional supplemental material is published online only. To view, please visit the journal online (http://dx.doi.org/10.1136/jitc-2022-005902).

LS, JL, DZ and MS contributed equally.

Accepted 02 January 2023

For numbered affiliations see end of article.

Correspondence to
Dr Yun Chen; chenyun@njmu.edu.cn

Dr Dongyan Shi; shidongyan@njmu.edu.cn

Dr Lin Lin; lin9100@aliyun.com

Dr Wen-Hui Li; 15189200969@163.com

ABSTRACT

Background Immune-checkpoint inhibitors (ICIs) remain ineffective in a large group of non-small cell lung cancer (NSCLC) patients. Mucosal-associated invariant T (MAIT) cells, a population of unconventional innate-like T lymphocytes abundant in the human body, play important roles in human malignancies. Little is known about the immune characteristics of MAIT cells in NSCLC and correlation with prognosis and response rate of ICIs treatment.

Methods To investigate the distribution, activation status, and function of MAIT cells in NSCLC patients and their correlations with anti-PD-1 immunotherapy, MAIT cells in peripheral blood, tumor and paratumor samples from NSCLC patients with or without anti-PD-1 immunotherapy were analyzed using flow cytometry and single-cell RNA-sequencing.

Results MAIT cells were enriched in the tumor lesions of NSCLC patients migrating from peripheral blood via the CCR6-CCL20 axis. Both peripheral and tumor-infiltrating MAIT cells displayed an exhausted phenotype with upregulated PD-1, TIM-3, and IL-17A while less IFN-γ. Anti-PD-1 therapy reversed the function of circulating MAIT cells with higher expression of IFN-γ and granzyme B. Subcluster MAIT-17s (defined as cells highly expressing exhausted and Th17-related genes) mainly infiltrated in the non-responsive tissues, while the subcluster MAIT-IFNGRs (cells expressing genes related to cytotoxic function) were mainly enriched in responsive tissues. Moreover, we found predictive value of circulating MAIT cells for anti-PD-1 immunotherapy in NSCLC patients.

Conclusions MAIT cells shifted to an exhausted tumor-promoting phenotype in NSCLC patients and the circulating MAIT subset could be a predictor for patients who respond to anti-PD-1 immunotherapy.

WHAT IS ALREADY KNOWN ON THIS TOPIC

⇒ Mucosal-associated invariant T (MAIT) cells have been proved to involve in innate immunity and play indispensable roles in malignancies. However, little is known about the immune characteristics of MAIT cells in non-small cell lung cancer (NSCLC) and its correlation with anti-PD-1 therapy.

WHAT THIS STUDY ADDS

⇒ In this study, MAIT cells were observed to be enriched in the tumor lesions via the CCR6-CCL20 axis and shift to an exhausted tumor-promoting phenotype in NSCLC patients. Furthermore, the circulating MAIT-IFNGR subset showed potential predictive value for the responders while MAIT-17 subset indicated resistance to anti-PD-1 therapy in NSCLC patients.

HOW THIS STUDY MIGHT AFFECT RESEARCH, PRACTICE OR POLICY

⇒ The transcriptional profiles of MAIT cells are impacted by the tumor microenvironment and showed potential predictive value for patients who respond to anti-PD-1 therapy.

BACKGROUND

Non-small cell lung cancer (NSCLC) representing 85% of lung cancer has become the leading cause of cancer-related deaths worldwide with low 5-year survival rates varying from 4% to 17%.[1] Cancer cells can escape from host immune surveillance through various pathways, such as disrupting T cell effectors and antitumor immunity. For patients with advanced NSCLC, immune-checkpoint inhibitors (ICIs) restimulate T cell activation by blocking the inhibitory interactions between T cells and tumor cells or dendritic cells, for example, programmed death-1 (PD-1)-programmed death ligand-1 (PD-L1).[2]

Anti-PD-1/PD-L1 antibodies were shown to improve overall survival in lung cancers, though, there remains a large group of patients that do not respond to PD-1/PD-L1 blockade, making it a formidable challenge to search for biomarkers that indicate whether the patients will respond to the therapy.[2–4] Detecting PD-L1 expression by immunohistochemistry is the most frequently used diagnostic test approved by FDA for ICIs. However, numerous studies have shown that many patients with PD-L1 positive tumors did not benefit from the PD-1/PD-L1 blockade therapy. Other biomarkers such as tumor mutational burden, tumor-infiltrating

lymphocytes, mismatch repair deficiency, and microsatellite instability also have limitations.[5]

Mucosal-associated invariant T (MAIT) cells are a population of innate-like T cells whose T cell receptor consists of an invariant α chain and varying β chains and restricts to the major histocompatibility complex (MHC) class I-related molecule (MR1). MAIT cells are enriched at mucosal locations as well as peripheral blood and tissues.[6] Once activated, they exert cytotoxic properties and produce inflammatory cytokines such as IFN-γ, TNF-α, and IL-17A, and cytotoxic mediators such as granzyme B and perforin. Studies have shown that MAIT cells were diminished in peripheral blood, enriched in the tumor lesions of patients with mucosal tumors (gastric cancer, colorectal cancer (CRC), and lung cancer), and suppressed antitumor immunity by producing protumor cytokines IL-17A and IL-8, which were considered as biomarkers to monitor and predict clinical benefit from ICIs in multiple patients with cancer.[7–9] Studies revealed that the tumor-promoting capacity of MAIT cells was IL-17A-dependent.[10] However, whether MAIT cells correlate with the prognosis of NSCLC and the response rate of ICIs treatment remains to be further explored.

In this study, we observed the enrichment of MAIT cells in the tumor lesions which was mainly mediated by the CCR6-CCL20 axis in NSCLCs. We identified the exhausted MAIT cells with increased IL-17A production which contribute to immunotherapy resistance. Of note, we distinguished MAIT-IFNGR subset, which highly increased in patients with NSCLC who responded to anti-PD-1 therapy and confirmed circulating MAIT-IFNGRs can identify the response patients, thereby showing potential value for predicting the prognosis and ICIs response in NSCLC patients.

MATERIALS AND METHODS

Patients and samples

This study cohort included 186 patients with NSCLC, 14 patients with CRC, 20 patients with esophageal carcinoma (ESCA), and 16 patients with stomach adenocarcinoma (STAD) in Jiangsu Cancer Hospital between 2018 and 2022, together with 24 age-matched and gender-matched healthy donors (HDs) who received routine physical examination. Detailed clinical characteristics are presented in online supplemental tables S1 and S2.

Flow cytometry analysis

Flow cytometry was optimized to broadly investigate MAIT cells' phenotype and function, including CD3, CD4, CD8, TCR Vα7.2, CD161, HLA-DR, CD38, PD-1, CTLA-4, TIM-3, IFN-γ, granzyme B, IL-17A, IL-8, Annexin V, Ki-67, CCR6, and IFN-γR. Detailed information is listed in online supplemental materials and methods and table S3.

Immunofluorescence

Paraffin-embedded specimens were stained with H&E, and immunofluorescence. Deparaffinized sections were hydrated and then incubated with specific antibodies. Positive cells were detected by confocal microscopy (Carl Zeiss LSM800 with NLO and Airyscan). Detailed information is provided in online supplemental materials and methods.

Statistical analysis

The number of biological replicates and technical repeats in each experimental group is indicated in the figure legends. Two-sided p ≤0.05 was considered statistically significant. All statistical analyses were performed using R (V.3.4.0) unless indicated otherwise. Detailed information is described in online supplemental materials and methods.

Additional methods are provided in the online supplemental materials and methods.

RESULTS

MAIT cells exhibit specific transcriptomic features in NSCLCs by Single-cell RNA sequencing

To explore the dynamics of immune cell populations potentially involved in the tumor microenvironment, we performed a secondary analysis of the published NSCLC single-cell RNA sequencing (scRNA-seq) dataset (14 patients from GSE99254, 11 patients from GSE162498),[11 12] with a focus on the abundance and the transcriptional profiles of MAIT cells from isolated $CD3^+$ T cells in peripheral blood, tumor and paratumor tissues. In these 25 patients, 20 patients were diagnosed with early-stage and 5 patients with advanced-stage NSCLC. The computational analysis identified 20 different cell clusters based on gene expression profiles (figure 1A). Among those, cluster 12 was identified as MAIT cells expressing high levels of *SLC4A10*, *IL18RAP*, *IL23R*, *NCR3*, *COLQ*, and *ME1* (figure 1B,C). It has been reported that MAIT cells with tumor-homing properties were identified with a high expression level of *KLRB1*, *SLC4A10*, *MAF*, and *CXCR4*,[13] which was similar to the expression pattern of genes in cluster 12 (figure 1D). MAIT cells also existed in peripheral blood, tumor, and paratumor tissues in multiple cancer species (online supplemental figure S1A–C and methods).[14–17] Notably, most MAIT cells were enriched in tumor tissues among different cancers (online supplemental figure S1D). We obtained a set of top 30 genes as MAIT cell-specific signatures (cluster 12) for the analysis of the TCGA database (online supplemental materials and methods). Our data showed that high infiltration of MAIT cells was significantly correlated with unfavorable disease-free survival in NSCLC patients (p=0.0029; figure 1E). To interrogate potential signaling pathways related to MAIT cells' function in NSCLC, we compared transcriptomic differences of MAIT cells between tumor and paratumor tissues. Kyoto Encyclopedia of Genes and Genomes (KEGG) signaling mechanism analysis

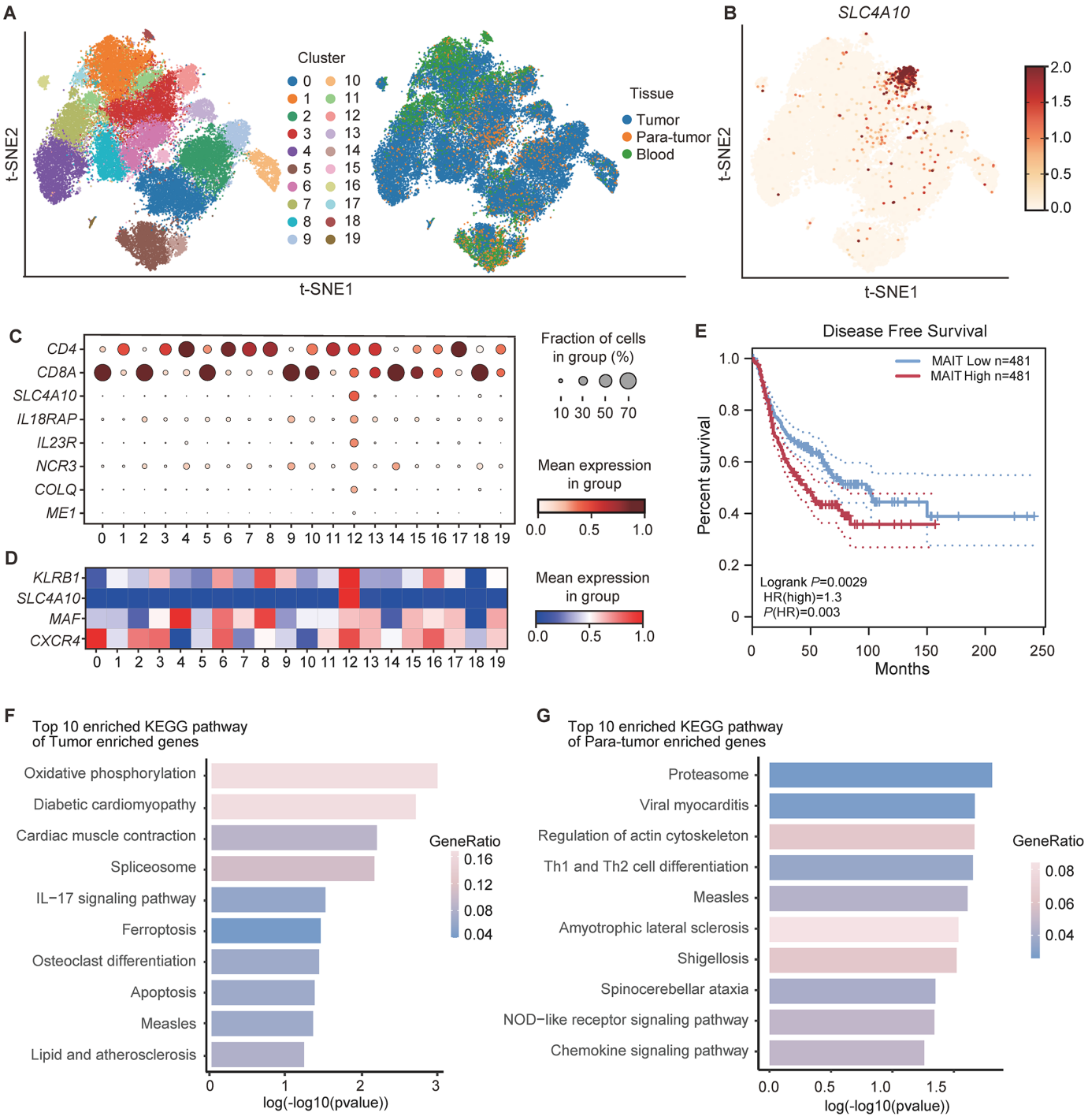

Figure 1 The abundance and transcriptional profiles of MAIT cells in non-small cell lung cancer (NSCLC) patients based on scRNA-seq data (14 patients from GSE99254 and 11 patients from GSE162498). (A) t-Distributed Stochastic Neighbor Embedding (t-SNE) plot displaying 20 clusters identified on the basis of gene expression levels of $CD3^+$ T cells in peripheral blood, tumor, and paratumor tissues from NSCLC patients. Cells are colored according to the 20 clusters defined in an unsupervised manner. (B) Expression of SLC4A10 in $CD3^+$ T cells from peripheral blood, tumor and paratumor tissues of NSCLC patients. (C) Dot plot for markers characterizing MAIT cells with tumor-homing properties in NSCLC patients. The color intensity of each dot corresponds to the average gene expression across all cells in each cluster. (D) Dot plot for selected markers characterizing mucosal-associated invariant T (MAIT) cells with tumor-homing properties (cluster 12) that were reported previously.[21] The color intensity of each dot corresponds to the average gene expression across all cells in each cluster. (E) Kaplan-Meier curves for disease-free survival (DFS) according to MAIT cell frequency in NSCLC patients from the TCGA database. (F) The top 10 enriched KEGG pathway of tumor enriched genes in MAIT cells from NSCLC patients. (G) The top 10 enriched KEGG pathway of paratumor enriched genes in MAIT cell from NSCLC patients. Survival analysis was determined by the log-rank (Mantel-Cox) test.

showed that tumor-enriched MAIT cells upregulated genes involved in IL-17 signaling pathways (figure 1F; online supplemental table S4), while MAIT cells in paratumor tissues, by contrast, upregulated genes involved in pathways of Th1 and Th2 cell differentiation (figure 1G; online supplemental table S5). A similar tendency was found in other cancer species (online supplemental figure S1E). These results suggested that there is a potential function bifurcation into Th17-like MAIT cells sublineage and Th1-like or Th2-like MAIT cells sublineage in NSCLC, consistent with prior studies.[18 19]

MAIT cells are significantly enriched in tumor tissues from NSCLC patients

To confirm the preferential tumor tissue tropism of MAIT cells in NSCLC patients, frequencies of $CD3^+$ $CD161^+$ TCR $V\alpha7.2^+$ MAIT cells (hereafter referred to as MAIT cells) in tumor and paratumor tissues were analyzed (figure 2A; online supplemental figure S2A and table S1). We observed a higher proportion of MAIT cells in $CD3^+$ T cells from tumor lesions compared with that from paratumor tissues (median (IQR) 1.07% (0.74%–1.47%) vs 0.75% (0.44%–1.27%), p=0.045; figure 2B,C). These findings were validated in 9 tumor and their paired paratumor tissues, which were part of total tissue samples from 90 patients (online supplemental table S1), where MAIT cells also increased in tumor tissues from NSCLC patients (p=0.027; online supplemental figure S2B). These MAIT cells were mainly CD8 positive (online supplemental figure S2C,D). Increased tumor-infiltrating MAIT cells were also visible via immunofluorescence staining in other cancer species (online supplemental figure S3A).

To figure out the origin of the increased tumor-infiltrating MAIT cells, we assessed the percentage of $Ki\text{-}67^+$ MAIT cells and revealed no difference between tumor and paired paratumor tissues (n=14) (figure 2D), indicating the proliferation rate of MAIT cells was not altered. Also, apoptosis did not differ significantly between the two groups by staining MAIT cells with Annexin V and 7-AAD (n=12) (figure 2E). Previous studies demonstrated that MAIT cells retained tissue enrichment properties might be explained by the specific chemokine receptor expression.[20 21] We next analyzed the mRNA expression of chemokines that recruit MAIT cells in tumor tissues from NSCLC and found the expression of CCL20 was elevated (p=0.037, figure 2F), in line with high levels of CCR6 on circulating MAIT cells as reported, which is the receptor of CCL20.[21 22] Increased expression of CCL20 in tumors compared with paratumor tissues was observed by ELISA (median (IQR), 1.303 (0.811–3.78) vs 0.403 (0.271–0.596), p<0.001, figure 2G) and immunofluorescence (MFI median (IQR), 9.83 (14.43–6.62) vs 3.83 (4.13–3.02), p<0.001; figure 2H,I) in NSCLC patients. Meanwhile, a similar chemokine pattern with a high level of CCL20 was confirmed by analysis of RNA-seq datasets from the TCGA database in multiple cancer species (online supplemental figure S3B–E). The expression of chemokine pattern in the tumor microenvironment may be of importance for organ-specific migration of MAIT cells.

MAIT cells gather in tumor tissues from peripheral blood via the CCR6-CCL20 axis in NSCLCs

Frequencies of MAIT cells in peripheral blood of NSCLC patients were reduced compared with that of HDs (median (IQR), 0.9% (0.41%–1.5%) vs 5.79% (4.17%–7.34%), p<0.001; figure 3A–C). However, there was no obvious difference in MAIT cell proliferation and apoptosis between 15 NSCLC patients and the control group of 14 healthy individuals (online supplemental figure S4A,B). To explore the mechanism of chemokine-mediated migration in MAIT cells, we used the single-cell RNA-seq data to identify differential expression of the chemokines/receptors in MAIT cells between tumor and paratumor or blood samples. There was no significant difference in *CCR6*, *CXCR6*, *CXCR4*, *CCR4*, *CCR5*, and *ITGA4*, which were previously reported to be expressed in MAIT cells (online supplemental figure S4C–F).[6] CCR6, the receptor of CCL20, was found highly expressed in MAIT cells (more than 80%) from peripheral blood mononuclear cells (PBMCs) or tissues using flow cytometry (online supplemental figure S4G,H). However, there was no difference in the levels of CCR6 between $CD8^+$ and $CD4^+$ MAIT cells (online supplemental figure S4I,J).

To further investigate the chemotactic effects of CCL20 on $CCR6^+$ MAIT cells, we next performed the MAIT cell chemotactic migration assay and flow cytometry to analyze the MAIT cells from PBMCs (figure 3D; supplemental materials and methods). A notable MAIT cell chemotaxis was observed when cultured with conditional medium that contained a relatively high concentration of CCL20 from NSCLC cell lines H1299 and PC9 (figure 3E). However, the chemotaxis response could be partially blocked by anti-CCL20 mAb (for H1299 medium, p=0.0022; for PC9 medium, p=0.0049). These results collectively suggested that circulating MAIT cells migrated to tumor tissues through the CCR6-CCL20 axis in NSCLC patients.

MAIT cells from PBMCs in NSCLCs mainly consist of exhausted IL-17A-secreting $CD8^+$ subset with impaired effector capability

The depletion of circulating MAIT cells was observed in patients with other cancer species, including ESCA, STAD, and CRC (online supplemental figure S5A,B). Generally, $CD8^+$ cells constituted more than 65% of total MAIT cells in peripheral blood from different cancers (online supplemental figure S5C). The proportion of these peripheral $CD8^+$ MAIT cells among total $CD3^+$ T cells was significantly decreased in NSCLC patients when compared with HDs (median (IQR), 0.68% (0.35%–1.22%) vs 4.04% (3.3%–5.3%), p<0.001; figure 3F–H). In contrast, the proportion of $CD4^+$ MAIT cells showed no alteration (figure 3H). Given some evidence suggesting that $CD8^+$ MAIT subset plays a specific role in the recognition of MR1-presented antigen and cytokines

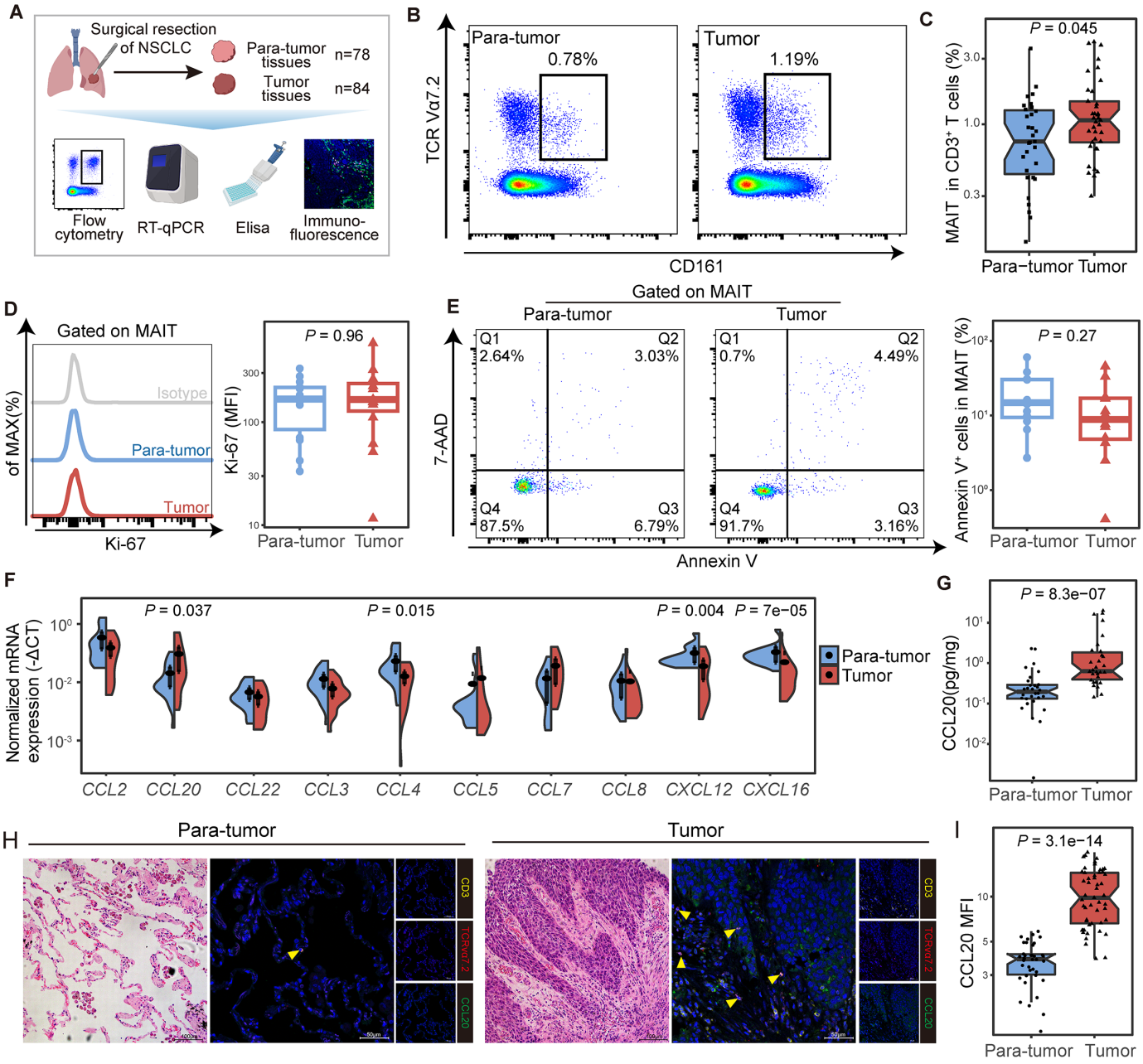

Figure 2 Mucosal-associated invariant T (MAIT) cells were enriched in tumor tissues potentially via the CCR6-CCL20 axis in non-small cell lung cancer (NSCLC) patients. (A) Scheme of the study design. Flow cytometry was applied to analyze MAIT cells distribution in tumor and paratumor tissues of patients with NSCLC. (B, C) Representative plots of MAIT cells (gated on $CD3^+$ $CD161^+$ TCR $V\alpha7.2^+$) in tumor and paratumor tissues of NSCLC patients and its summary data (paratumor, n=31; tumor, n=37). (D) Representative plots of Ki-67 expression in MAIT cells from tumor and paratumor tissues of NSCLC patients and its summary data (n=14). (E) Representative Annexin V/7-ADD dot plots that demonstrate the percentage of apoptotic MAIT cells in tumor and para-tumor tissues of NSCLC patients and its summary data (n=12). (F) Relative expressions of chemokines that recruit MAIT cells in tumor and para-tumor tissues of NSCLC patients (n=20) using quantitative real-time PCR (RT-qPCR). (G) Expression of CCL20 in paired tumor and paratumor tissues of NSCLC patients (n=30) by ELISA. (H, I) Tumor and paratumor tissue sections were stained with hematoxylin and eosin (HE) (left) and immunofluorescence staining for CD3, TCR Vα7.2, and CCL20 (right) and its summary data. Immunofluorescence was performed on paired paratumor and tumor tissues from 7 NSCLC patients. Each dot represents one individual high-power field. Scale bar, 100 µm or 50 µm. The upper and lower ends of the boxes represented IQR of values. The lines in the boxes represented median value. Statistical significance was calculated via Mann-Whitney U test.

production,[23–25] we inferred that MAIT cells underwent potential function alteration in NSCLC patients.

Next, we performed polychromic flow cytometry to probe MAIT cells for features of immune activation and exhaustion. MAIT cells from PBMCs in patients with NSCLC showed significantly higher levels of the activation marker HLA-DR and CD38 (for HLA-DR median (IQR), 12% (7.65%–20.6%) vs 3.9% (1.05%–8.96%), p<0.001;

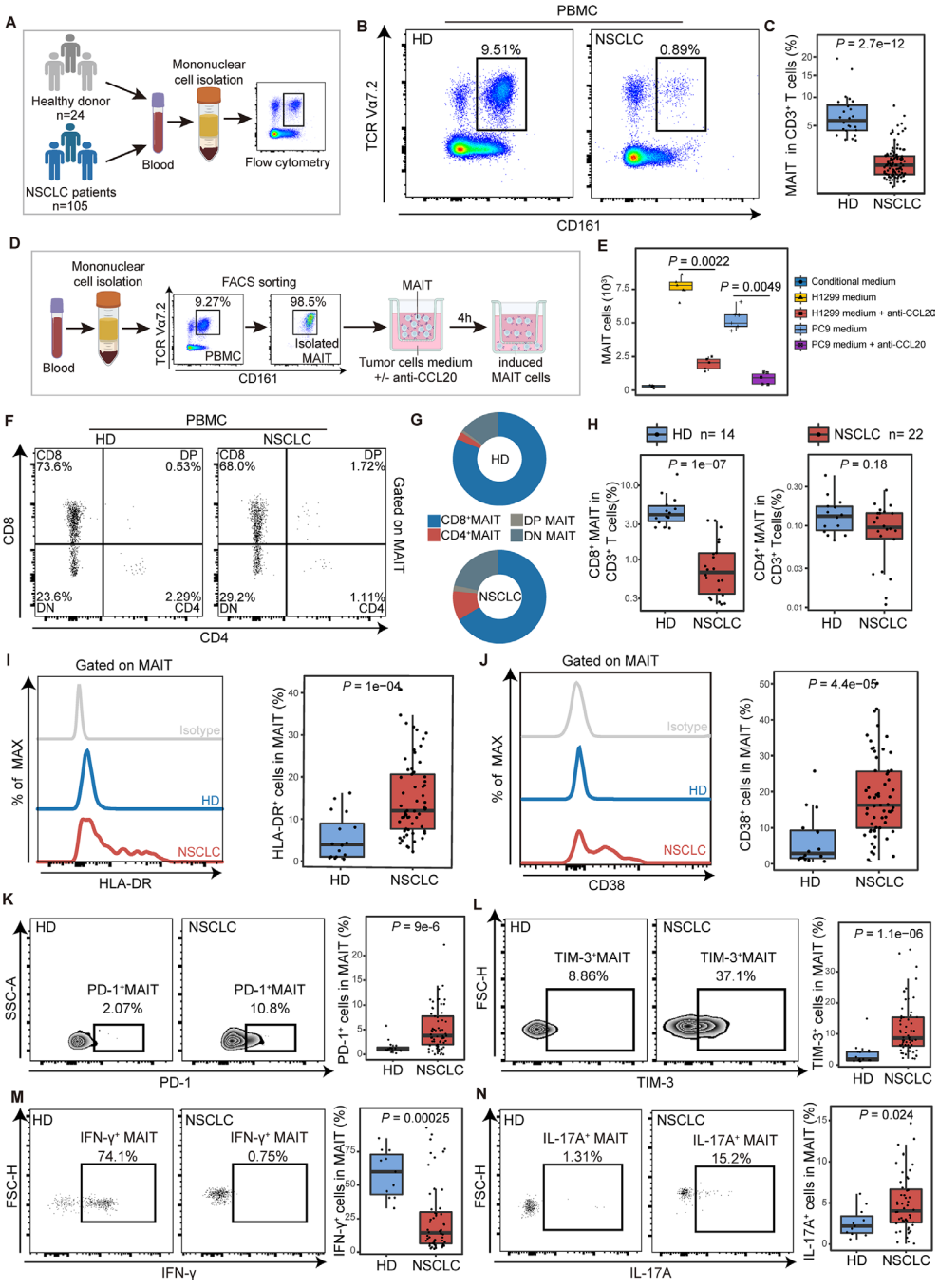

Figure 3 The chemotaxis and functional phenotype of mucosal-associated invariant T (MAIT) cells from PBMCs in non-small cell lung cancer (NSCLC) patients. (A) Scheme of the study design. Flow cytometry was applied to analyze MAIT cells from PBMCs of healthy donors (HD) and NSCLC patients. (B and C) Representative plots of MAIT cells (gated on $CD3^+CD161^+TCR\ V\alpha7.2^+$) in peripheral blood of healthy donors and NSCLC patients and its summary data. (HD, n=16; NSCLC, n=61). (D) Flow chart of in vitro MAIT cell chemotactic migration assay. The purity of isolated MAITs is shown. (E) Summary data of MAIT cell migration treated with or without the neutralizing antibody (±anti-CCL20) in the bottom. MAIT cells (10^3) induced in each condition were evaluated (n=6). (F) Representative plots of MAIT cell subsets (gated on $CD3^+$ $CD161^+$ TCR $V\alpha7.2^+$) from PBMCs of healthy donors (HD) and NSCLC patients. (G) MAIT cell subset composition in peripheral blood of HD and NSCLC patients. (H) Quantification of $CD8^+$ MAIT cells and $CD4^+$ MAIT cells in $CD3^+$ T cells in peripheral blood of HD and NSCLC patients. (HD, n=14; NSCLC, n=22). (I and J) Expression of the activation markers HLA-DR and CD38 on MAIT cells from PBMCs of HD and NSCLC patients detected by FCM (gated on $CD3^+$ $CD161^+$ TCR $V\alpha7.2^+$) and their summary data. (HD, n=16; NSCLC, n=61). (K and L) Expression of the immune inhibitory molecules PD-1 and TIM-3 on MAIT cells from PBMCs of HD and NSCLC patients detected by FCM (gated on $CD3^+$ $CD161^+$ TCR $V\alpha7.2^+$) and their summary data. (HD, n=16; NSCLC, n=61). (M and N) Expression of the effector molecules IFN-γ and IL-17A in MAIT cells from PBMCs of HD and NSCLC patients detected by FCM (gated on $CD3^+$ $CD161^+$ TCR $V\alpha7.2^+$) after stimulated with PMA and ionomycin for 4 hours and their summary data. (HD, n=11; NSCLC, n=52). The upper and lower ends of the boxes represented IQR of values. The lines in the boxes represented median value. Statistical significance was calculated via Mann-Whitney U test. PBMC, peripheral blood mononuclear cells.

for CD38, 16.3% (10%–25.6%) vs 2.89% (1.56%–9.26%), p<0.001, figure 3I,J), indicating that circulating MAIT cells were chronically activated T-cell phenotype.[26 27] Significant upregulation of PD-1 and TIM-3 on MAIT cells from PBMCs was detected in NSCLC patients compared with that in HDs (for PD-1 median (IQR), 4.57% (2.72%–7.51%) vs 1.12% (0.78%–1.43%), p<0.001; for TIM-3, 8.08% (4.92%–15%) vs 1.84% (1.45%–4.17%), p<0.001; figure 3K,L). Although the expression of CTLA-4 showed no difference (online supplemental figure S6A), these MAIT cells from NSCLC patients represent a phenotype consistent with exhausted cells by coexpressing PD-1 with TIM-3.[28 29] In chronic infections and cancer, the exhausted T cells are often associated with the deterioration of effector function.[30 31] Thus, we used flow cytometry to determine whether the ability of PD-1$^+$TIM-3$^+$ MAIT cells to produce cytokines and the cytotoxicity was affected. After being stimulated with phorbol-12-myristate-13-acetate (PMA) and ionomycin for 4 hours, the IFN-γ-secreting ability of MAIT cells from PBMCs of NSCLC patients was significantly lower compared with that in HDs (median (IQR), 14.05% (6.43%–30.62%) vs 60% (43.15%–72.9%), p<0.001; figure 3M). Nevertheless, the IL-17A- secreting ability was found elevated in MAIT cells from PBMCs in NSCLCs (median (IQR), 4.19% (2.84%–6.71%) vs 2.34% (1.5%–3.54%), p=0.024; figure 3N), which was reported to possess potential protumor effects in different cancers.[32 33] Granzyme B production in response to such stimulation remained unchanged in MAIT cells from PBMCs (online supplemental figure S6B). The level of IL-8, which is considered as a tumor-promoting cytokine,[8] was also upregulated (median (IQR), 4.87% (2.49%–7.83%) vs 1.47% (0.96%–3.05%), p=0.008; online supplemental figure S6C). ScRNA-seq analysis reveals the expression level of *IFNG* (encoding IFN-γ) was negatively correlated with *HAVCR2* (encoding TIM-3) (r=−0.01, p=0.007), while *IL17A* expression was positively correlated with *HAVCR2* (r=0.08, p=5.8e-8) and *PDCD1* (encoding PD-1) (r=0.39, p=2.2e-16) (online supplemental figure S6D). We then verified that PD-1$^+$ MAIT cells lead to a significant decrease in the level of IFN-γ (r=−0.339, p=0.017; online supplemental figure S6E) using flow cytometry. Of note, exhausted MAIT cells (PD-1$^+$TIM-3$^+$) produce IL-17 (r=0.211, p=0.024) (online supplemental figure S6F). Thus, these results indicate that NSCLC represents an alteration in the function of MAIT cells with the contribution of IL-17 but only little IFN-γ. A similar tendency of immune characteristics in MAIT cells from NSCLC continues in other cancer species (online supplemental figure S7).

Tumor-infiltrating MAIT cells exhibit exhausted phenotype different from those in paratumor

To investigate the characteristics of MAIT cells in the tumor microenvironment, we detected the phenotype of infiltrating MAIT cells from adjacent paratumor (n=27) and tumor (n=34) tissues in NSCLC patients by flow cytometry and immunofluorescence. The clinicopathological characteristics of the patients are detailed in online supplemental table S1, and the workflow is shown in online supplemental figure S8A. Higher expression of CD38 was observed in tumor-infiltrating MAIT cells than that in paratumor tissues (median (IQR), 10.15% (6.39%–18.23%) vs 4.72% (2.5%–6.24%), p<0.001; figure 4A), while the level of HLA-DR showed no difference (online supplemental figure S6B). Consistent with the previous findings from PBMCs, the expression of PD-1 and TIM-3 were increased in tumor-derived MAIT cells compared with their counterparts in paratumor tissues (for PD-1 median (IQR), 17.65% (8.81%–30.1%) vs 7.23% (2.7%–15.17%), p=0.0076; for TIM-3, 7.05% (3.73%–8.64%) vs 2.72% (1.73%–5.58%), p=0.032; figure 4B and C). Granzyme B and IFN-γ production was inhibited in tumor tissues (for granzyme B median (IQR), 10.6% (6.28%–14.43%) vs 14.8% (10.25%–32.8%), p=0.0063; for IFN-γ, 5.79% (4.22%–14.67%) vs 12.8% (10.9%–21.45%), p=0.0037; figure 4D and E), while the IL-17A- secreting ability elevated (median (IQR), 7% (4.65%–10.72%) vs 4.22% (2.25%–6.74%), p=0.013; figure 4F). The expression of CTLA-4 and IL-8 in MAIT cells between paratumor and tumor showed no difference (online supplemental figure S8C,D). We further confirmed the elevated PD-1$^+$ and IL-17A$^+$ tumor-enriched MAIT cells microscopically using immunofluorescence (figure 4G,H). Additionally, we observed upregulated HLA-DR, CD38, PD-1, TIM-3, IL-17A, and downregulated IFN-γ, granzyme B in MAIT cells in the analysis of 15 tumors and their paired paratumor samples, which were part of the total tissue samples from NSCLC patients (online supplemental figure S8E–M). Collectively, these data revealed that tumor-infiltrating MAIT cells displayed exhausted phenotype and impaired effector abilities in NSCLC patients.

Circulating MAIT cells with cytotoxic effect show predictive value for response to anti-PD-1 therapy

Previous studies have reported that IL-17A could direct tumor immune escape and even promote resistance to anti-PD-1 therapy in multiple cancers.[7 33] Given exhausted MAIT cells produced high levels of IL-17A (figures 3N and 4F), and were related to poor outcomes (figure 1E), we assumed the feature of circ-MAIT cells may be considered as a biomarker to predict the success of PD-1 blockade therapy, which is clinically detectable before ICIs. A total of 105 peripheral blood samples were collected from patients with NSCLC pre (n=35) or post (n=70) anti-PD-1 treatment, including 10 samples from patients diagnosed at the early stage (stages I/II) and 95 samples from the advanced stage (stages III/IV) (online supplemental table S2). No significant difference in the frequency of MAIT cells was observed in patients pre (n=23) and post (n=38) PD-1 blockade treatment (online supplemental figure S9A). Next, we assessed the immune characteristics of MAIT cells and found there is no difference in the activation (HLA-DR and CD38) and exhaustion (PD-1, TIM-3 and CTLA-4) phenotypes of MAIT cells in post-treatment versus pretreatment samples

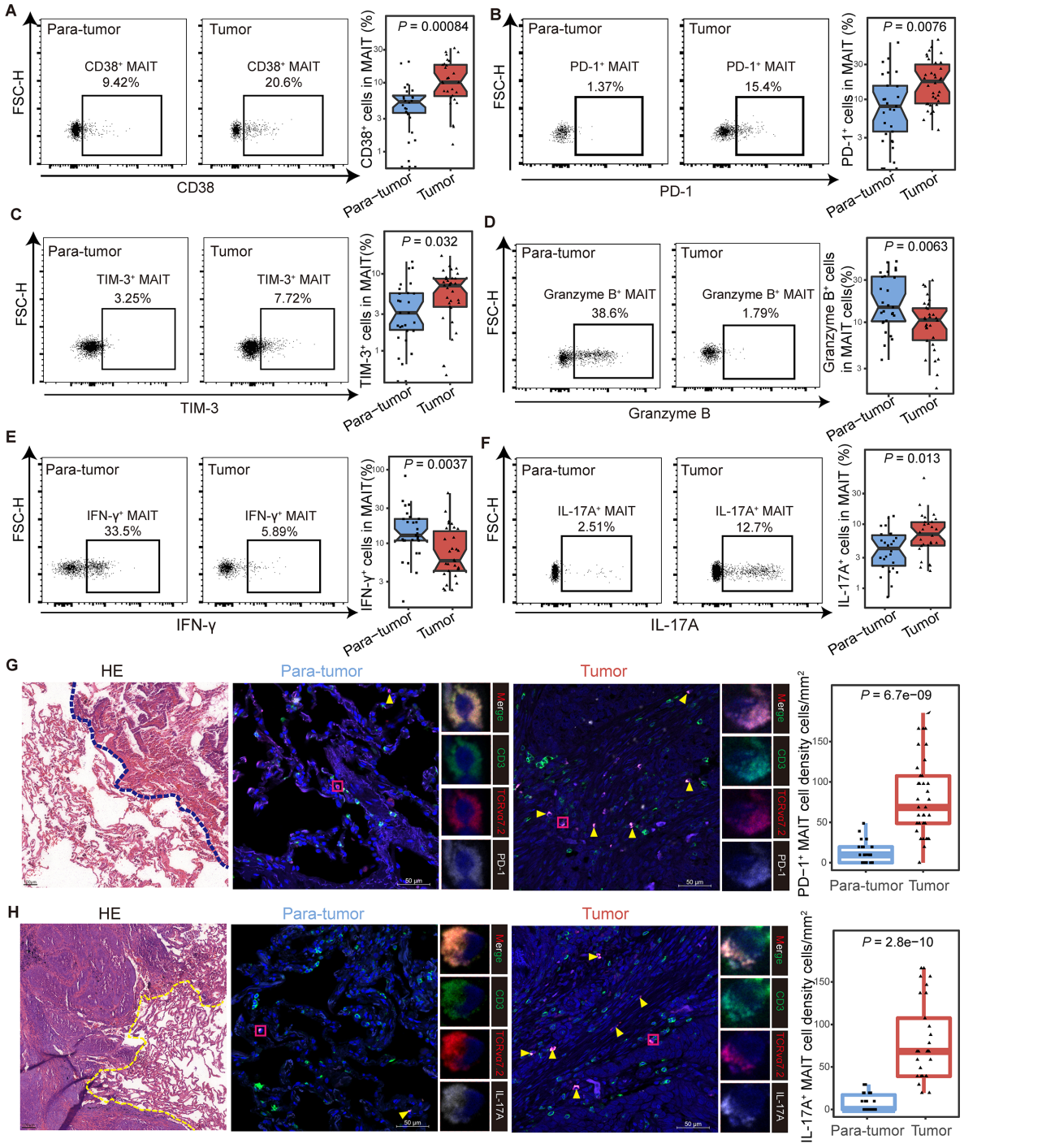

Figure 4 Functional phenotype of tumor-infiltrating mucosal-associated invariant T (MAIT) cells in non-small cell lung cancer (NSCLC) patients. (A) Expression of the activation marker CD38 on MAIT cells from tumor and para-tumor tissues of NSCLC patients detected by FCM (gated on $CD3^+$ $CD161^+$ TCR $V\alpha7.2^+$) and its summary data. (Paratumor, n=27; tumor, n=28). (B and C) Expression of the immune inhibitory molecules PD-1 (B) and TIM-3 (C) on MAIT cells from tumor and paratumor tissues of NSCLC patients detected by FCM (gated on $CD3^+$ $CD161^+$ TCR $V\alpha7.2^+$) and their summary data. (Paratumor, n=27; tumor, n=34). (D–F) Expression of the effector molecules granzyme B (D), IFN-γ (E) and IL-17A (F) in MAIT cells from tumor and para-tumor tissues of NSCLC patients detected by FCM (gated on $CD3^+$ $CD161^+$ TCR $V\alpha7.2^+$) after stimulated with PMA and ionomycin for 4 hours and their summary data. (Paratumor, n=27; tumor, n=30). (G) Tumor and paratumor tissue sections were stained with hematoxylin and eosin (left) and immunofluorescence staining for CD3, TCR Vα7.2, and PD-1 (right) and summary of density information of $PD\text{-}1^+$ MAIT cells. Scale bar, 50 µm. (H) Tumor and paratumor tissue sections were stained with H&E (left) and immunofluorescence staining for CD3, TCR Vα7.2, and IL-17A (right) and summary of density information of $IL\text{-}17A^+$ MAIT cells. Immunofluorescence was performed on paired paratumor and tumor tissues from 5 NSCLC patients. Each dot represents one individual high-power field. Scale bar, 100 µm or 50 µm. The upper and lower ends of the boxes represented IQR of values. The lines in the boxes represented median value. Statistical significance was calculated via Mann-Whitney U test. FCM, flow cytometry; PMA, phorbol-12-myristate-13-acetate.

(online supplemental figure S9B–F). However, the expression of granzyme B was elevated (median (IQR), 11.4% (4.782%–20.075%) vs 3.87% (3.13%–65.26%), p=0.00038), but IL-17A decreased (median (IQR), 3.28% (2.095%–3.911%) vs 5.03% (3.815%–6.500%), p=0.004) in MAIT cells from the patients after PD-1 blockade treatment (online supplemental figure S9G,H). No significant difference was observed in the expression of IFN-γ and IL-8 in MAIT cells (online supplemental figure S9I,J).

We further divided the patients into pretreatment, post-treatment with progressive disease (PD), stable disease (SD), partial response or complete response (PR/CR) according to Response Evaluation Criteria in Solid Tumors (RECIST) (version 1.1). The frequency of MAIT cells remained unchanged in patients with PD, SD, and PR/CR (online supplemental figure S9K). We observed upregulation of HLA-DR in PR/CR patients compared with SD and pretreatment patients (median (IQR), 18.8% (12.9%–24.68%) vs 10.5% (6.05%–13.4%) or 11% (7.31%%–15.2%), p=0.0081 or p=0.013, respectively; figure 5A). PD-1$^+$ MAIT cells were significantly decreased in PR/CR patients compared with the SD, PD or pretreatment patients (median (IQR), 2.52% (1.17%–5.15%) vs 5.35% (4%–9.77%) or 8.4% (5.38%–17.7%) or 5.04% (3.71%–8.82%), p=0.0026 or p<0.001 or p=0.0025, respectively; figure 5B). When it came to cellular function effector, we found increased granzyme B and IFN-γ following anti-PD-1 therapy in PR/CR patients compared with SD or pretreatment patients (for granzyme B median (IQR), 2.52% (1.17%–5.15%) vs 5.78% (3.45%–8.54%) or 4% (3.59%%–5.31%), p=0.006 or p=0.0011; for IFN-γ, 35.95% (14.9%–74.28%) vs 13.05% (4.32%–26.58%) or 9.93% (5.88%–15.95%), p=0.04 or p=0.0025, respectively; figure 5C and D). IL-17A, though, was reduced in PR/CR patients compared with pretreatment patients (median (IQR), 2.98% (1.89%–5.82%) vs 4.92% (3.15%–6.4%), p=0.028, respectively; figure 5E). Thus, these results indicated that PD-1 blockade did not affect the frequency of MAIT cells, but benefits from immunotherapy depended on the MAIT cell function to some extent.

Subcluster MAIT-IFNGRs predict response while MAIT-17s indicate resistance to anti-PD-1 therapy in NSCLC patients

Lung cancer is a highly heterogeneous cancer type. To explore the landscape of MAIT cells in the microenvironment of NSCLC during ICI therapy, we took advantage of the scRNA-seq dataset profiling immune cells within paired NSCLC tumor samples pre and post anti-PD-1 therapy from Caushi *et al* (GEO accessions GSE176022).[34] MAIT cells were further subclustered before comparing the responders (R) (n=6) and non-responders (NR) (n=8) during anti-PD-1 therapy (figure 6A). We applied the miloR tool to quantify shifts in the abundance of MAIT cells between responders and non-responders, identifying 351 neighborhoods spanning the KNN graph (k=30), of which 91 showed evidence of differential abundance (false discovery rate (FDR) = 25%) (online supplemental figure S10A). Two different subclusters of MAIT cells were identified that MAIT-IFNGR subcluster was mainly enriched in responders while MAIT-17 subcluster was prevalent in the non-responders (figure 6B,C). Notably, similar to cluster MAIT-IFNGR in figure 6B, the cluster 0 of MAIT cells we analyzed before (online supplemental figure S4F) also displayed high expression of *IFNGR1*, suggesting a potential role for these cells in antitumor immunity and response to immunotherapy.

We next compared the transcriptomic profiles between the two subclusters (figure 6D and online supplemental table S6). We observed that subcluster MAIT-17 (mainly non-responders), highly expressed *IL17A* and immune checkpoint receptors, such as *PDCD1*, and *ENTPD1(CD39)*, together with genes-inducing exhaustion programs like *TOX*.[35 36] By contrast, subcluster MAIT-IFNGR (mainly responders) tended to express genes related to immune-cell activation (*RIPOR2, CD6, TYROBP*), effector (*IFNGR1, NKG7, LITAF*), and cytotoxic function (*GZMA, GZMK, GZMM, PRF1, GNLY*) (figure 6D). What is more, we examined the differences in signal pathways of these two MAIT subsets (figure 6E). Cluster MAIT-IFNGR was highly enriched in positive regulation of cell activation, T cells activation, and lymphocyte adhesion, consistent with a better prognosis for ICIs. Cluster MAIT-17, nevertheless, was enriched in negative regulation of cell activation, and myeloid leukocyte differentiation, which might account for the clinical resistance to anti-PD-1 therapy.[37 38]

Circulating MAIT-IFNGR subset could be a clinically accessible predictor for NSCLC patients responsive to anti-PD-1 immunotherapy

We next evaluated the MAIT-IFNGR and MAIT-17 subsets in the peripheral blood of patients receiving anti-PD-1 therapy, with the characteristics of high expression of IFN-γR and PD-1, respectively. Thirty-one samples were newly collected to validate the IFN-γR$^+$ MAIT cells (NR, n=17; R, n=14) (online supplemental table S2). IFN-γR$^+$ MAITs within CD3$^+$ T cells were significantly increased in the responders (patients with PR/CR) compared with non-responders (patients with PD/SD) while PD-1$^+$ MAITs decreased (for IFN-γR$^+$ MAITs median (IQR), 0.17% (0.08%–0.67%) vs 0.05% (0.04%–0.14%), p=0.0079; for PD-1$^+$ MAITs, 0.04% (0.01%–0.07%) vs 0.05% (0.03%–0.11%), p=0.041; online supplemental figure S10B,C). When it came to effectors, the IFN-γR$^+$ granzyme B$^+$ MAIT subset was expanded and the PD-1$^+$ IL-17A$^+$ MAIT subset reduced (median (IQR), 1.45% (1.03%–2.68%) vs 0.76% (0.49%–1.18%), p=0.026; 0.2% (0.07%–0.3%) vs 0.58% (0.33%–0.8%), p=0.0026; respectively; figure 6F,G). Notably, we included a typical patient who responded and later became resistant to immunotherapy. Tumor tissues were sampled via informed consent and tracked the detailed clinical data, including CT (figure 6H,I). We explicitly revealed increased infiltration of MAIT-IFNGR cells in responding tumor lesion 1, whereas the MAIT-17 signatures diminished (figure 6J and online supplemental figure S10D). Meanwhile, non-responding tumor lesion two exhibited a significant increase in MAIT-17 cells while

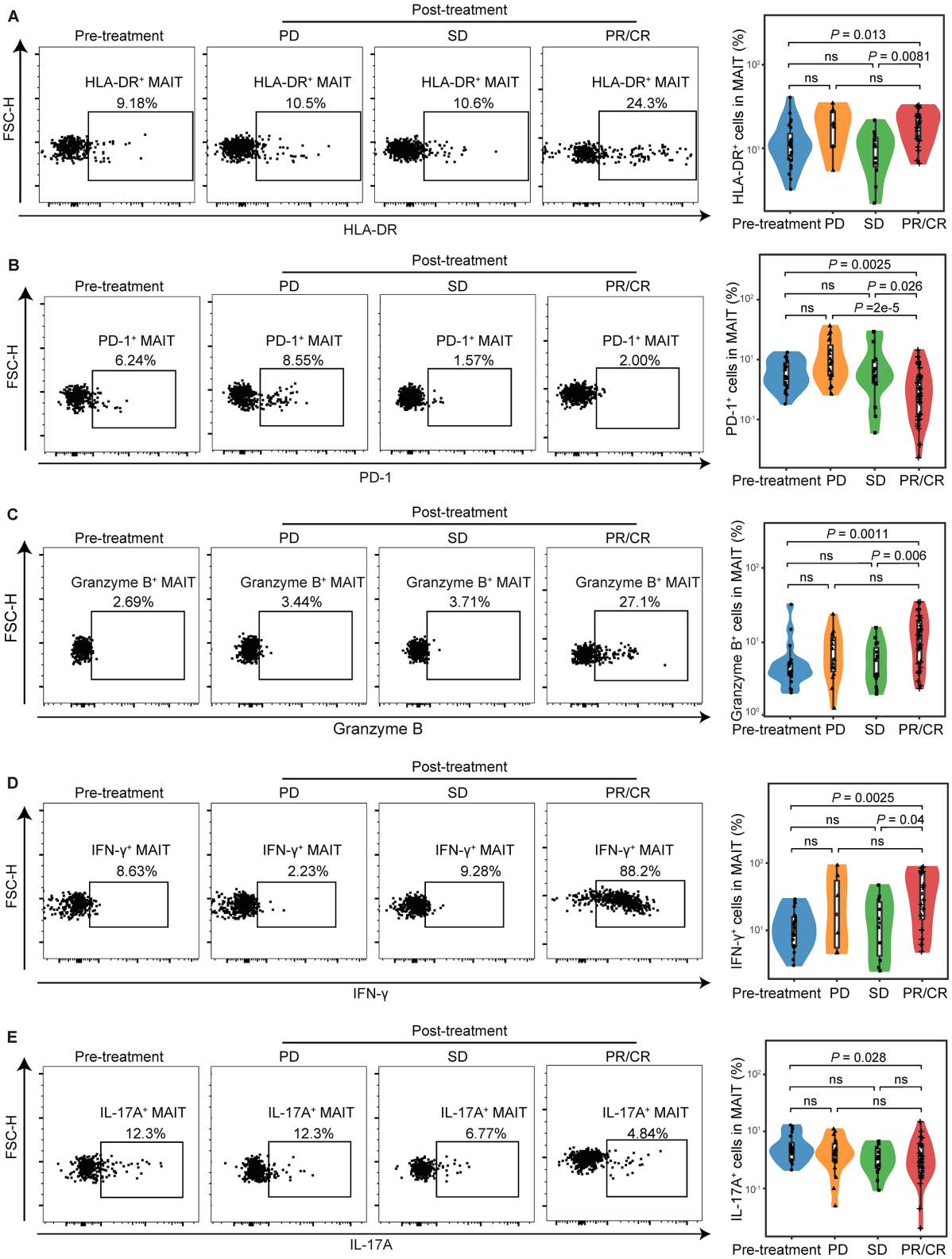

Figure 5 Functional alterations of circulating mucosal-associated invariant T (MAIT) cells in non-small cell lung cancer (NSCLC) patients who responded to anti-PD-1 therapy. Expression of HLA-DR (A), PD-1 (B), granzyme B (C), and IFN-γ (D), and IL-17A (E) in MAIT cells from peripheral blood of pretreatment NSCLC patients (HLA-DR, PD-1, n=26; IFN-γ, granzyme B, IL-17A, n=20), patients with progressive disease (PD) (HLA-DR, n=8; PD-1, n=18; IFN-γ, n=6; granzyme B, n=18; IL-17A, n=15), patients with stable disease (SD) (HLA-DR, n=11; PD-1, n=15; IFN-γ, n=11; granzyme B, IL-17A, n=15) and patients with complete response or partial response (CR/PR) (HLA-DR, n=18; PD-1, n=31; IFN-γ, n=16; granzyme B, IL-17A, n=29) detected by FCM (gated on $CD3^+$ $CD161^+$ TCR $V\alpha7.2^+$) and their summary data. The upper and lower ends of the boxes represented IQR of values. The lines in the boxes represented median value. Statistical significance was calculated via Mann-Whitney U test or one-way ANOVA and Tukey multiple comparison tests. ANOVA, analysis of variance.FCM, flow cytometry.

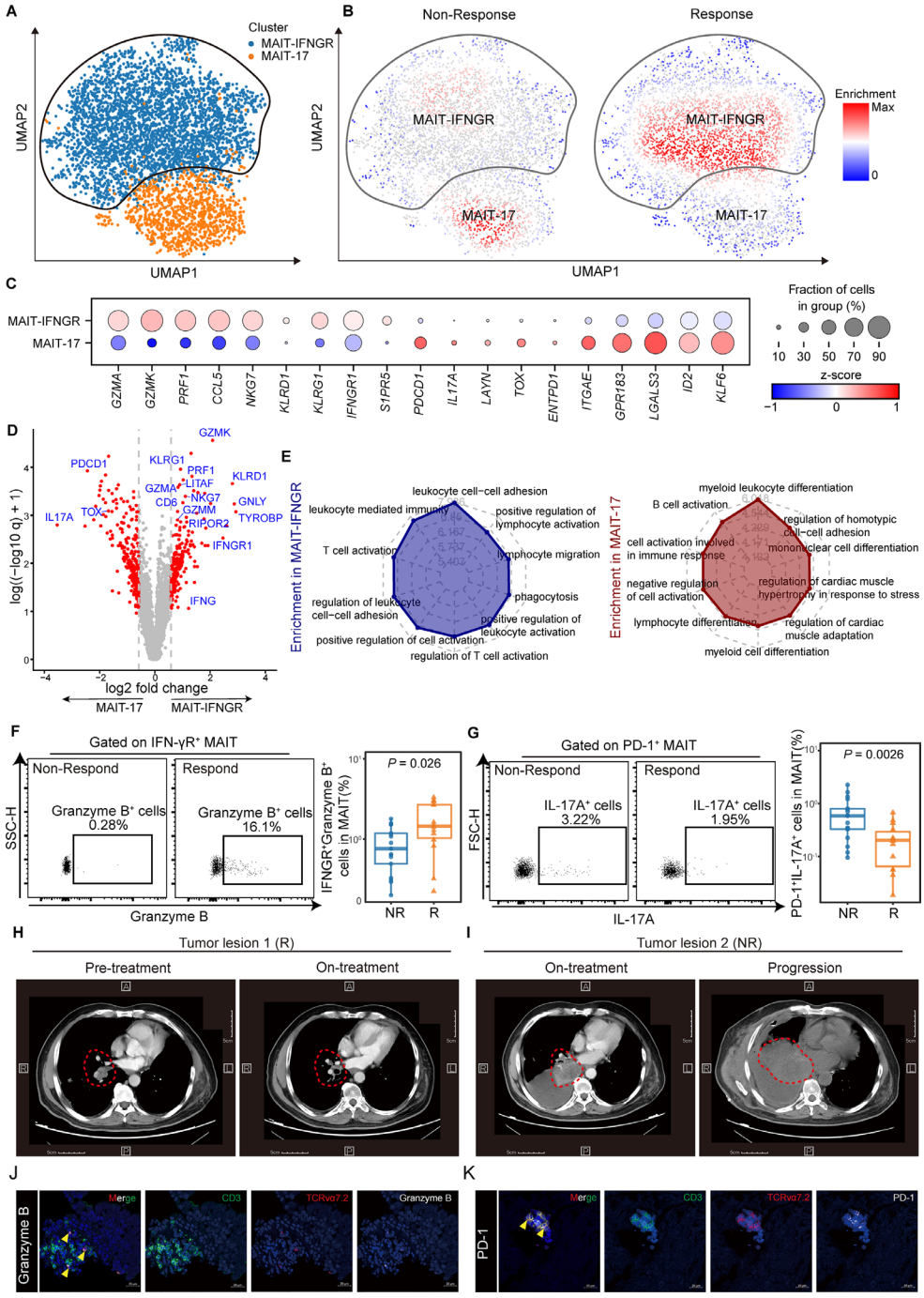

Figure 6 Mucosal-associated invariant T (MAIT) cells can be devided into two different subclusters and are associated with immune-checkpoint inhibitor (ICI) responsiveness. (A) UMAP (uniform manifold approximation and projection) plot displaying two subclusters identified on the basis of gene expression levels of MAIT cells from paired non-small cell lung cancer (NSCLC) tumor tissues pre-anti-PD-1 and post-anti-PD-1 therapy (GSE176022). Cells are colored according to the two subclusters defined in an unsupervised manner. (B) UMAP plot displaying MAIT cell subclusters enrichment in tumor tissues from the responders (R, n=6) and non-responders (NR, n=8). (C) Dot plot for markers characterizing MAIT-IFNGR and MAIT-17 cells in NSCLC tumor tissues. The color intensity of each dot corresponds to the z-score across all cells in each cluster. (D) Volcano plot showing differentially expressed genes between the MAIT-17 and MAIT-IFNGR subclusters. Each red dot denotes an individual gene with adjusted q<0.05 and fold change >1.5. (E) Radar chart for gene enrichment in MAIT-IFNGR and MAIT-17. (F) Expression of granzyme B on tumor-infiltrating IFN-γR $^+$ MAIT cells of NSCLC patients who received anti-PD-1 therapy detected by FCM (gated on CD3$^+$ CD161$^+$ TCR Vα7.2$^+$ IFN-γR$^+$) and its summary data (NR, n=17; R, n=14). (G) Expression of IL-17A on tumor-infiltrating PD-1$^+$ MAIT cells of NSCLC patients who received anti-PD-1 therapy detected by FCM (gated on CD3$^+$ CD161$^+$ TCR Vα7.2$^+$ PD-1$^+$) and its summary data (NR, n=17; R, n=14).(H and I) CT scan of NSCLC patient who received anti-PD-1 therapy. Respective tumor tissue sections were immunofluorescence stained with anti-CD3, TCR Vα7.2, granzyme B (J), and PD-1 (K). Scale bar, 20 µm. The upper and lower ends of the boxes represented the IQR of values. The lines in the boxes represented the median value. Statistical significance was calculated via Mann-Whitney U test.

the MAIT-IFNGR signature was dismissed (figure 6K and online supplemental figure S10E). Our data demonstrated that circulating MAIT-IFNGR cell subsets with anti-tumor effector functions and cytotoxic capabilities could predict the responders while the MAIT-17s indicate resistance to anti-PD-1 therapy in NSCLC patients.

DISCUSSION

Innate immunity plays an important role in antitumor immune responses, among which MAIT cells are a population of innate type T cells preferentially enriched in human mucosal tissue, indicating its potential role in lung cancer, which involves mucosal immunity.[39] In this study, we identified the feature of circulating and infiltrating MAIT cells in patients with NSCLC and revealed the potential ability of MAIT cells to be a biomarker for patients responding to anti-PD-1 therapy.

Altered phenotype and cytokine production patterns have been reported in different cancer types, and even in the same case of HCC, controversial data existed on the prognostic benefit of MAIT cells.[6] Our data reveal MAITs were enriched in tumor tissues, indicated poor outcomes and expressed transcriptomic profiles related to IL17 signaling pathways. Studies have shown the depletion of circulating MAIT cells in a variety of solid tumors, including cervical, colorectal, gastric, kidney cancers, and hepatocellular carcinoma.[20 40–43] Consistently, we observed the overall decrease of circulating MAIT cell frequency and the enrichment in tumor lesions in NSCLCs. Of note, HLA-DR$^+$ tumor-infiltrating MAIT cells increased particularly in paired tissue samples and it was not the case in unpaired statistics. Relatively small sample sizes and different individual backgrounds might cause this inconsistent result. Some previous studies demonstrated that reduced circulating MAIT cells might be explained by the specific chemokine receptor expression and their tissue-homing properties.[20 21] Our data revealed that NSCLC tissue expressed higher CCL20 (the ligand for CCR6), in line with high levels of CCR6 expression in circulating MAIT cell.[6 22] Flow cytometry, ELISA, immunofluorescence, analysis of scRNA-seq transcriptomic datasets displayed similar results. Taken together, CCR6-expressing MAIT cells from PBMCs could be recruited into the tumor lesions, which release high levels of the chemokine CCL20 in NSCLC patients. The chemotactic migration assay indicated that the CCR6-CCL20 axis was involved in the migration of cells into the tumors in NSCLC patients.

Murine MAIT cells could experience functional bifurcation into the IFN-γ-producing T-bet$^+$ Th1-like or the IL-17A-producing RORγt$^+$ Th17-like sub-lineage,[6 18 19] and Th17-polarized MAIT cells has been proposed to potentially promote the progression of multiple tumors associated with poor prognosis.[44 45] More work is needed to characterize the features of MAIT cells in malignancies. Hence, we evaluated MAIT cells from NSCLCs and confirmed these cells displayed an exhausted IL-17A-secreting CD8$^+$ MAIT subset with upregulated PD-1 and TIM-3, producing tumor-promoting cytokines like IL-8.[9 32]

Exhaustion has since become evident in infections and tumors and is sustained by the expression of inhibitory receptors with changes in transcription profiles.[46] Our analyses revealed the exhausted IL-17A-producing MAIT cells correlated with reduced functional capacity and poor prognosis. Prior studies have noted that IL-17A could increase the expression of PD-L1, promote tumor immune escape and even boost resistance to anti-PD-1 therapy in HCC, ovarian cancer, and microsatellite stable CRC.[7 33 47] IL-8, known as a tumor-promoting factor,[32] was also evaluated as a biomarker of response to anti-PD-1 immunotherapy in melanoma and NSCLC patients.[8 9] In this study, we found tumor microenvironment inflicts exhaustion of MAIT cells, and anti-PD-1 therapy could reinvigorate MAIT cells' antitumor effector functions. Accordingly, whether MAIT cells could be considered as a predictive marker of successful anti-PD-1 therapy aroused our great interest.

Two studies shared similar results that specific MAIT subsets represent a potential novel prognostic correlate of successful ICI therapy in melanoma patients undergoing anti-PD-1 therapy.[21 48] Throughout the flow cytometry and scRNA-seq data reanalysis, we defined and observed that MAIT-17s tend to enhance immunotherapy resistance in NSCLC while MAIT-IFNGRs inversely predicted successful ICIs. We further observed expanding circ-MAIT-IFNGR cells with restored effector functions and cytotoxic capabilities in NSCLC patients responding to anti-PD-1 therapy. Together with the homing properties of the MAIT cell, it is reasonable to confirm that the characteristics of MAIT cells in the peripheral blood could be considered as a predictive biomarker for response rate of PD-1 blockade.

As we acknowledge, some limitations associated with this study, such as the lack of a further meticulous mechanism that accounted for the alteration of MAIT cells, we revealed the characteristics of MAIT cells in NSCLCs and provided evidence of the association between different MAIT subsets and the response rate of ICIs in NSCLC. Meanwhile, because there were not enough cells we obtained from NSCLC patients to detect and quantify the characteristics of MAIT cells, the number of samples is not the same, despite being from the same cohort. Given the new techniques for expanding MAIT cells with antigen in vitro and vivo,[19] the use of 5-OP-RU, 6-FP,[49] and other ligands may offer the potential to further explore the role and mechanism of MAIT cells in the tumor microenvironment.

Author affiliations
[1]Department of Medical Oncology, Jiangsu Cancer Hospital, Jiangsu Institute of Cancer Research, Nanjing Medical University Affiliated Cancer Hospital, Nanjing, China
[2]Department of Immunology, Key Laboratory of Human Functional Genomics of Jiangsu Province, Gusu School, Nanjing Medical University, Nanjing, China

[3]Jiangsu Key Lab of Cancer Biomarkers, Prevention and Treatment, Collaborative Innovation Center for Cancer Personalized Medicine, Nanjing Medical University, Nanjing, China
[4]Department of Geriatrics, The First Affiliated Hospital of Nanjing Medical University, Nanjing, China
[5]Department of Hepatobiliary Surgery, The Yancheng School of Clinical Medicine of Nanjing Medical University, The Third People's Hospital of Yancheng, Yancheng, China
[6]Department of Gastroenterology, The First Affiliated Hospital of Nanjing Medical University, Nanjing, China

Contributors YC is responsible for the overall content as guarantor. YC conceived and designed the project. JL, DZ, MS, and JL performed experiments. LS, JL, WY, W-HL, and LL analysis and interpretation. YC, DZ, and DS drafting the manuscript for important intellectual content.All authors read and approved the manuscript.

Funding Supported by grants from the National Natural Science Foundation of China (82071767, 82171781, 82230059),Jiangsu Provincial Key Research Development Program of China (BE202277), and The Open Project of Jiangsu Biobank of Clinical Resources (SBK202004001).

Competing interests No, there are no competing interests.

Patient consent for publication Not applicable.

Ethics approval Study protocols were approved by the Human Research Ethics Committee of Jiangsu Cancer Hospital (Jiangsu, China) and carried out according to standard guidelines. Ethics ID: 2018-051. Participants gave informed consent to participate in the study before taking part.

Provenance and peer review Not commissioned; externally peer reviewed.

Data availability statement Data are available in a public, open access repository. All data relevant to the study are included in the article or uploaded as online supplemental information.

ORCID iD
Yun Chen http://orcid.org/0000-0002-4118-362X

REFERENCES

1 Hirsch FR, Scagliotti GV, Mulshine JL, *et al*. Lung cancer: current therapies and new targeted treatments. *Lancet* 2017;389:299–311.
2 Doroshow DB, Sanmamed MF, Hastings K, *et al*. Immunotherapy in non-small cell lung cancer: facts and hopes. *Clin Cancer Res* 2019;25:4592–602.
3 Niu M, Yi M, Li N, *et al*. Predictive biomarkers of anti-PD-1/PD-L1 therapy in NSCLC. *Exp Hematol Oncol* 2021;10:18.
4 Peters S, Kerr KM, Stahel R. PD-1 blockade in advanced NSCLC: a focus on pembrolizumab. *Cancer Treat Rev* 2018;62:39–49.
5 Rizvi NA, Hellmann MD, Snyder A, *et al*. Cancer immunology. mutational landscape determines sensitivity to PD-1 blockade in non-small cell lung cancer. *Science* 2015;348:124–8.
6 Godfrey DI, Koay H-F, McCluskey J, *et al*. The biology and functional importance of MAIT cells. *Nat Immunol* 2019;20:1110–28.
7 Liu C, Liu R, Wang B, *et al*. Blocking IL-17A enhances tumor response to anti-PD-1 immunotherapy in microsatellite stable colorectal cancer. *J Immunother Cancer* 2021;9:e001895.
8 Sanmamed MF, Perez-Gracia JL, Schalper KA, *et al*. Changes in serum interleukin-8 (IL-8) levels reflect and predict response to anti-PD-1 treatment in melanoma and non-small-cell lung cancer patients. *Ann Oncol* 2017;28:1988–95.
9 Schalper KA, Carleton M, Zhou M, *et al*. Elevated serum interleukin-8 is associated with enhanced intratumor neutrophils and reduced clinical benefit of immune-checkpoint inhibitors. *Nat Med* 2020;26:688–92.
10 Yan J, Allen S, McDonald E, *et al*. MAIT cells promote tumor initiation, growth, and metastases via tumor MR1. *Cancer Discov* 2020;10:124–41.
11 Guo X, Zhang Y, Zheng L, *et al*. Global characterization of T cells in non-small-cell lung cancer by single-cell sequencing. *Nat Med* 2018;24:978–85.
12 Gueguen P, Metoikidou C, Dupic T, *et al*. Contribution of resident and circulating precursors to tumor-infiltrating CD8$^+$ T cell populations in lung cancer. *Sci Immunol* 2021;6:eabd5778.
13 Sade-Feldman M, Yizhak K, Bjorgaard SL, *et al*. Defining T cell states associated with response to checkpoint immunotherapy in melanoma. *Cell* 2018;175:998–1013.
14 Azizi E, Carr AJ, Plitas G, *et al*. Single-cell map of diverse immune phenotypes in the breast tumor microenvironment. *Cell* 2018;174:1293–308.
15 Borcherding N, Vishwakarma A, Voigt AP, *et al*. Mapping the immune environment in clear cell renal carcinoma by single-cell genomics. *Commun Biol* 2021;4:122.
16 Zhang Q, He Y, Luo N, *et al*. Landscape and dynamics of single immune cells in hepatocellular carcinoma. *Cell* 2019;179:829–45.
17 Kürten CHL, Kulkarni A, Cillo AR, *et al*. Investigating immune and non-immune cell interactions in head and neck tumors by single-cell RNA sequencing. *Nat Commun* 2021;12:7338.
18 Koay H-F, Gherardin NA, Enders A, *et al*. A three-stage intrathymic development pathway for the mucosal-associated invariant T cell lineage. *Nat Immunol* 2016;17:1300–11.
19 Rahimpour A, Koay HF, Enders A, *et al*. Identification of phenotypically and functionally heterogeneous mouse mucosal-associated invariant T cells using MR1 tetramers. *J Exp Med* 2015;212:1095–108.
20 Won EJ, Ju JK, Cho Y-N, *et al*. Clinical relevance of circulating mucosal-associated invariant T cell levels and their anti-cancer activity in patients with mucosal-associated cancer. *Oncotarget* 2016;7:76274–90.
21 De Biasi S, Gibellini L, Lo Tartaro D, *et al*. Circulating mucosal-associated invariant T cells identify patients responding to anti-PD-1 therapy. *Nat Commun* 2021;12:1669.
22 Meermeier EW, Harriff MJ, Karamooz E, *et al*. MAIT cells and microbial immunity. *Immunol Cell Biol* 2018;96:607–17.
23 Dias J, Boulouis C, Gorin J-B, *et al*. The CD4$^-$CD8$^-$ MAIT cell subpopulation is a functionally distinct subset developmentally related to the main CD8$^+$ MAIT cell pool. *Proc Natl Acad Sci U S A* 2018;115:E11513–22.
24 Brozova J, Karlova I, Novak J. Analysis of the Phenotype and Function of the Subpopulations of Mucosal-Associated Invariant T Cells. *Scand J Immunol* 2016;84:245–51.
25 Kurioka A, Jahun AS, Hannaway RF, *et al*. Shared and distinct phenotypes and functions of human CD161++ Vα7.2+ T cell subsets. *Front Immunol* 2017;8:1031.
26 Zheng B, Wang D, Qiu X, *et al*. Trajectory and functional analysis of PD-1 ^{high} CD4 $^+$ CD8 $^+$ T cells in hepatocellular carcinoma by single-cell cytometry and transcriptome sequencing. *Adv Sci* 2020;7:2000224.
27 Philip M, Fairchild L, Sun L, *et al*. Chromatin states define tumour-specific T cell dysfunction and reprogramming. *Nature* 2017;545:452–6.
28 Egelston CA, Avalos C, Tu TY, *et al*. Human breast tumor-infiltrating CD8$^+$ T cells retain polyfunctionality despite PD-1 expression. *Nat Commun* 2018;9:4297.
29 Jin H-T, Anderson AC, Tan WG, *et al*. Cooperation of Tim-3 and PD-1 in CD8 T-cell exhaustion during chronic viral infection. *Proc Natl Acad Sci U S A* 2010;107:14733–8.
30 Zajac AJ, Blattman JN, Murali-Krishna K, *et al*. Viral immune evasion due to persistence of activated T cells without effector function. *J Exp Med* 1998;188:2205–13.
31 Philip M, Schietinger A. CD8$^+$ T cell differentiation and dysfunction in cancer. *Nat Rev Immunol* 2022;22:209–23.
32 Coussens LM, Zitvogel L, Palucka AK. Neutralizing tumor-promoting chronic inflammation: a magic bullet? *Science* 2013;339:286–91.
33 Wei Y, Shi D, Liang Z, *et al*. IL-17A secreted from lymphatic endothelial cells promotes tumorigenesis by upregulation of PD-L1 in hepatoma stem cells. *J Hepatol* 2019;71:1206–15.
34 Caushi JX, Zhang J, Ji Z, *et al*. Transcriptional programs of neoantigen-specific TIL in anti-PD-1-treated lung cancers. *Nature* 2021;596:126–32.

35 Khan O, Giles JR, McDonald S, *et al*. TOX transcriptionally and epigenetically programs CD8$^+$ T cell exhaustion. *Nature* 2019;571:211–8.
36 Scott AC, Dündar F, Zumbo P, *et al*. TOX is a critical regulator of tumour-specific T cell differentiation. *Nature* 2019;571:270–4.
37 Li K, Shi H, Zhang B, *et al*. Myeloid-derived suppressor cells as immunosuppressive regulators and therapeutic targets in cancer. *Signal Transduct Target Ther* 2021;6:362.
38 Loeuillard E, Yang J, Buckarma E, *et al*. Targeting tumor-associated macrophages and granulocytic myeloid-derived suppressor cells augments PD-1 blockade in cholangiocarcinoma. *J Clin Invest* 2020;130:5380–96.
39 Provine NM, Klenerman P. MAIT cells in health and disease. *Annu Rev Immunol* 2020;38:203–28.
40 Ling L, Lin Y, Zheng W, *et al*. Circulating and tumor-infiltrating mucosal associated invariant T (MAIT) cells in colorectal cancer patients. *Sci Rep* 2016;6:20358.
41 Huang W-C, Hsiao Y-C, Wu C-C, *et al*. Less circulating mucosal-associated invariant T cells in patients with cervical cancer. *Taiwan J Obstet Gynecol* 2019;58:117–21.
42 Duan M, Goswami S, Shi J-Y, *et al*. Activated and exhausted MAIT cells foster disease progression and indicate poor outcome in hepatocellular carcinoma. *Clin Cancer Res* 2019;25:3304–16.
43 Peterfalvi A, Gomori E, Magyarlaki T, *et al*. Invariant Valpha7.2-Jalpha33 TCR is expressed in human kidney and brain tumors indicating infiltration by mucosal-associated invariant T (MAIT) cells. *Int Immunol* 2008;20:1517–25.
44 Haeryfar SMM, Shaler CR, Rudak PT. Mucosa-associated invariant T cells in malignancies: a faithful friend or formidable foe? *Cancer Immunol Immunother* 2018;67:1885–96.
45 Zumwalde NA, Haag JD, Gould MN, *et al*. Mucosal associated invariant T cells from human breast ducts mediate a Th17-skewed response to bacterially exposed breast carcinoma cells. *Breast Cancer Res* 2018;20:111.
46 Wherry EJ, Kurachi M. Molecular and cellular insights into T cell exhaustion. *Nat Rev Immunol* 2015;15:486–99.
47 Aotsuka A, Matsumoto Y, Arimoto T, *et al*. Interleukin-17 is associated with expression of programmed cell death 1 ligand 1 in ovarian carcinoma. *Cancer Sci* 2019;110:3068–78.
48 Vorwald VM, Davis DM, Van Gulick RJ, *et al*. Circulating CD8$^+$ mucosal-associated invariant T cells correlate with improved treatment responses and overall survival in anti-PD-1-treated melanoma patients. *Clin Transl Immunology* 2022;11:e1367.
49 Eckle SBG, Birkinshaw RW, Kostenko L, *et al*. A molecular basis underpinning the T cell receptor heterogeneity of mucosal-associated invariant T cells. *J Exp Med* 2014;211:1585–600.